# Numerical Analyses of Discrete Gust Response for a Flexible Aircraft

Guowei YANG[1] and Shigeru OBAYASHI[2]
Tohoku University, Sendai 980-8577, Japan

**ABSTRACT**

Based on Navier-Stokes equations and structural and flight dynamic equations of motion, dynamic responses in vertical discrete gust flow perturbation are investigated for a supersonic transport model. A tightly coupled method was developed by the subiteration between aerodynamic equations and dynamic equations of motion. First, under the assumption of rigid-body and single freedom of motion in the vertical plunging, the results of direct-coupling method are compared with the results of quasi-steady model method. Then gust responses for the one-minus-cosine gust profile are analyzed with two freedoms of motion in plunging and pitching for the rigid and flexible airplane configurations.

## 1. Introduction

Gust load is one of the important dynamic loads considered in aircraft structure design. Due to its multidisciplinary nature with aerodynamics, flight dynamics, aeroelasticity and atmospheric turbulence, up to now, only the doublet-lattice, unsteady linear aerodynamic code (DLM) coupled with the equation of motion of flexible vehicle was used for the gust response analysis [1-3].

Gusts in nature tend to random. The early design methods for gust loads were based on a single discrete gust having one-minus-cosine velocity profile. Recently the statistical discrete gust (SDG) method and the power spectral density (PSD) method [4] in the frequency domain are used to define the gust loads, however, which are still difficult to combine with the modern Navier-Stokes numerical method.

In the paper, the fully implicit multiblock Navier-Stokes aeroelastic solver implemented by the authors [5], coupled with the flight and structural dynamic equations of motion, has been developed to simulate gust dynamic responses for the supersonic transport (SST) designed by National Aerospace Laboratory of Japan (NAL) [6]. To study the effects of dynamic response due to flow perturbation and airplane motion, only the consideration of vertical plunging motion, a comparative study was first done for the rigid airplane in the harmonic flow perturbation with the direct-coupling method and the quasi-steady model method. Then the gust responses in a one-minus-cosine gust velocity profile are analyzed with two freedoms of motion in plunging and pitching for the rigid and flexible airplane models.

## 2. Aerodynamic Equations and Numerical Method

Aerodynamic governing equations are the unsteady, three-dimensional thin-layer Navier-Stokes equations in strong conservation law form, which can be written in curvilinear coordinates as

$$\partial_t \hat{Q} + \partial_\xi F + \partial_\eta G + \partial_\zeta H = \partial_\zeta H_v + S_{GCL} \qquad (1)$$

The source term $S_{GCL}$ is obtained from the geometric conservation for a moving mesh [7]. In the formulation, all variables are normalized by the appropriate combination of freestream density, freestream velocity and mean aerodynamic chord length. The viscosity coefficient $\mu$ in $H_v$ is computed as the sum of laminar and turbulent viscosity coefficients, which are evaluated by the Sutherland's law and Baldwin-Lomax model [8].

LU-SGS method [9], employing a Newton-like subiteration, is used for solving Eq. 1. Second order temporal accuracy is obtained by utilizing three-point backward difference in the subiteration procedure. The numerical algorithm can be deduced as

[1]Present position: Professor, Institute of Mechanics, Chinese Academy of Sciences, 100080 Beijing, China.
[2]Professor, Institute of Fluid Science, Associate Fellow AIAA

$$
\begin{aligned}
&LD^{-1}U\Delta Q \\
&= -\phi^i\{(1+\phi)Q^p - (1+2\phi)Q^n + \phi Q^{n-1} \\
&- J\Delta t Q^p S_{GCL}^p + J\Delta t(\delta_\xi F^p + \delta_\eta G^p + \delta_\zeta (H^p - H_v^p))\}
\end{aligned} \tag{2}
$$

where

$$L = \overline{\rho} I + \phi^i J\Delta t(A^+_{i-1,j,k} + B^+_{i,j-1,k} + C^+_{i,j,k-1})$$

$$D = \overline{\rho} I$$

$$U = \overline{\rho} I - \phi^i J\Delta t(A^-_{i+1,j,k} + B^-_{i,j+1,k} + C^-_{i,j,k+1})$$

and

$$\overline{\rho} = 1 + \phi^i J\Delta t(\overline{\rho}(A) + \overline{\rho}(B) + \overline{\rho}(C))$$

$$\phi^i = 1/(1+\phi)$$

$$\Delta Q = Q^{p+1} - Q^p$$

Here $\phi = 0.5$ and $Q^p$ is the subiteration approximation to $Q^{n+1}$. As $p \to \infty$, $Q^p \to Q^{n+1}$. The deduced subiteration scheme reverts to the standard first-order LU-SGS scheme for $\phi = 0$ and $p = 1$.

The inviscid terms in Eq. 1 are approximated by the modified third-order upwind HLLEW scheme of Obayashi et al [10]. For the isentropic flow, the scheme results in the standard upwind-biased flux-difference splitting scheme of Roe, and as the jump in entropy becomes large in the flow, the scheme turns into the standard HLLE scheme. Thin-layer viscous term in Eq. 1 is discretized by second-order central difference.

For multiblock-grid application, the Navier-Stokes equations are solved in each block separately. To calculate the convective and viscous fluxes in the block boundary, data communication is performed through two-level halo cells. The detail about the multiblock Navier-Stokes solver can be found in references [5] [11].

## 3. Equations of Motion and Numerical Method

In the present study of dynamic response, the airplane is permitted freedom in vertical plunging and pitching, and the following assumptions are made,

1. The disturbed motion is symmetrical with respect to the airplane's longitudinal plane of symmetry.
2. The airplane is initially in horizontal flight at cruise velocity.
3. The vertical gust perturbation is normal to the flight path, and is uniform in the spanwise direction.
4. For the flexible analyses, only the structural deformation of the wing is considered and its deformation is approximated to the elastic plate model.

### 3.1 Direct-coupling method

With the above assumptions, the equilibriums of total force along the z-axis and total pitching moment about the y-axis are:

$$\iint_S \ddot{w}(x,y,t)\rho dxdy = \iint_S \Delta p(x,y,t)dxdy \tag{3a}$$

$$\iint_S \ddot{w}(x,y,t)\rho x dxdy = \iint_S \Delta p(x,y,t)x dxdy \tag{3b}$$

For the equilibrium of an element, we obtain:

$$
\begin{aligned}
&w(x,y,t) - w(0,0,t) - x\frac{\partial w(0,0,t)}{\partial x} \\
&= \iint_S C(x,y;\xi,\eta)[\Delta p(\xi,\eta,t) - \rho(\xi,\eta)\ddot{w}(\xi,\eta,t)]d\xi d\eta
\end{aligned} \tag{3c}
$$

In the system of equations, the unknown quantity is $w(x,y,t)$, which represents the disturbed displacement of elastic airplane from its original equilibrium state. The pressure change of $\Delta p(x,y,t)$ based on cruise condition is calculated by the aerodynamic equations, which depends on the instantaneous values of displacement, velocity, acceleration of airplane, as well as the past history of the motion.

Introducing natural modes with the Rayleigh-Ritz method [12], we have,

$$w(x,y,t) = \sum_{i=1}^{n} \phi_i(x,y) q_i(t) \tag{4}$$

where $\phi_i(x,y)$ is normalized natural mode shapes of the airplane including rigid modes and $q_i(t)$ generalized displacement. Then Equations (3a-3c) can be deduced to

$$\ddot{q}_i + 2\zeta_i \omega_i \dot{q}_i + \omega_i^2 q_i = F_i / M_i \tag{5}$$

$$(i = 1,2,\cdots,n; \omega_1 = \omega_2 = 0)$$

with the initial conditions $q_i(0) = \dot{q}_i(0) = 0$ and where

$$M_i = \iint_S \phi_i^2(x,y)\rho(x,y)dxdy$$

$$F_i = \iint_S \Delta p(x, y, t)\phi_i(x, y)dxdy$$

The first equation in Eq. 5 is the equation of motion in vertical plunging. In the equation, the generalized mass $M_1$ represents the mass of airplane, and $q_1$ the plunging displacement. Similarly, the second equation is the equation of motion in pitching. $M_2, q_2$ represent the pitching moment of inertia and angular displacement in pitching, respectively. $\omega_i$ , $\varsigma_i$ are the natural frequency of structural modes and the damping ratio in the $i$ th mode, which are 0 for the first two equations.

The subiteration method can also be used for Eq. 5. The resulting numerical scheme is

$$\begin{aligned}&\begin{bmatrix} 1 & -\phi^i \Delta t \\ \phi^i \Delta t \omega_i^2 & 1+2\phi^i \omega_i \zeta_i \Delta t \end{bmatrix} \Delta S \\ &= -\phi^i \{(1+\phi)S^p - (1+2\phi)S^n + \phi S^{n-1} \\ &+ \Delta t \begin{bmatrix} 0 & -1 \\ \omega_i^2 & 2\omega_i \zeta_i \end{bmatrix} S^p - \Delta t \begin{bmatrix} 0 \\ F_i^p / M_i \end{bmatrix} \}\end{aligned} \tag{6}$$

where $S = [q, \dot{q}]$, $\Delta S = S^{p+1} - S^p$.

As $p \to \infty$, a full implicit second-order temporal accuracy scheme for the numerical simulation of dynamic response is formed by the coupling solutions of Eqs. 2 and 6. Numerical experiments [13] indicate, in general, the calculated results are nearly unchangeable as $p \geq 3$. In the following calculation, the number of subiteration is set to 3.

If the airplane is assumed as the rigid body, then only the first two equations of Eq. 5 coupled with the aerodynamic equations are needed. If the pitching motion can be further neglected, the dynamic response is only considered in the motion of vertical plunging. For the simpler case, the quasi-steady model method can be introduced as follows.

### 3.2 Quasi-steady model method

If the time lag in the lift increase is neglected and the incremental lift is considered only due to the change of angle of attack, then the model equation of motion can be written simply as,

$$M\ddot{z} = \frac{1}{2}\rho_\infty V_\infty^2 S C_{L\alpha}\left(\frac{w(t)}{V_\infty} - \frac{\dot{z}}{V_\infty}\right) \tag{7}$$

where $w(t)$ represents the vertical perturbation velocity profile. The normalized equation can be written as:

$$\ddot{z} + C_1 C_{L\alpha}\dot{z} = C_1 C_{L\alpha} w(t) \tag{8}$$

where $C_1 = \dfrac{\rho_\infty Sc}{2M}$

$C_{L\alpha}$ is the derivative of lift coefficient which can be determined by a steady flow calculation or wind tunnel experiment. Through the comparison of this method with the direct-coupling method, the dynamic responses under the quasi-steady assumption can be studied.

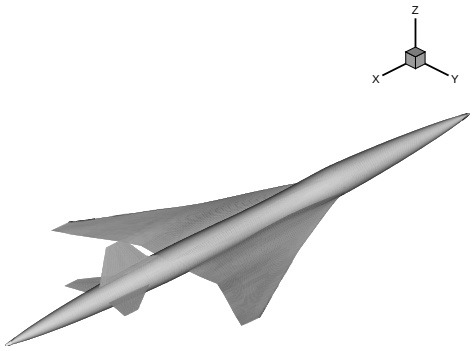


**Fig. 1 SST configuration**

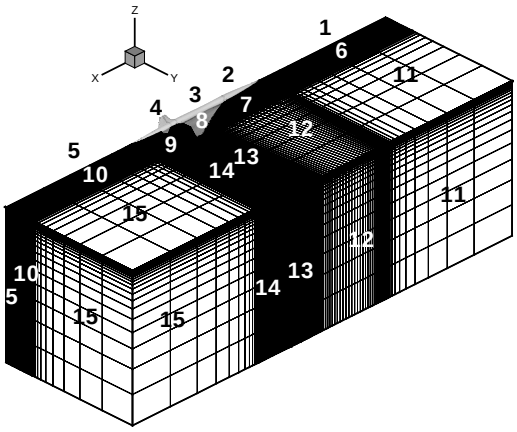


**Fig. 2 Multiblock grid with 30 blocks for SST**

## 4. Results and Discussions

Dynamic responses in vertical flow perturbation are studied for the SST experimental model [6] shown in Fig. 1. For the experimental aircraft, the fuselage length is 11.5m, the mean aerodynamic chord 2.754m, the reference area $S = 10.12m^2$, the weight 1950kg, the center of gravity from the nose of the airplane 6.05266m and the pitching moment of inertia $I_{yy} = 10632kgm^2$.

The design cruise point is at $M_\infty = 2.0$, $\alpha = 2°$ and $\mathrm{Re} = 27.5\times10^6$, and the flight altitude 15,000m. The aircraft is initially assumed at cruise flight, and then encounters a gust turbulence atmosphere. So the calculation of gust dynamic response needs to start from the cruise steady flowfield.

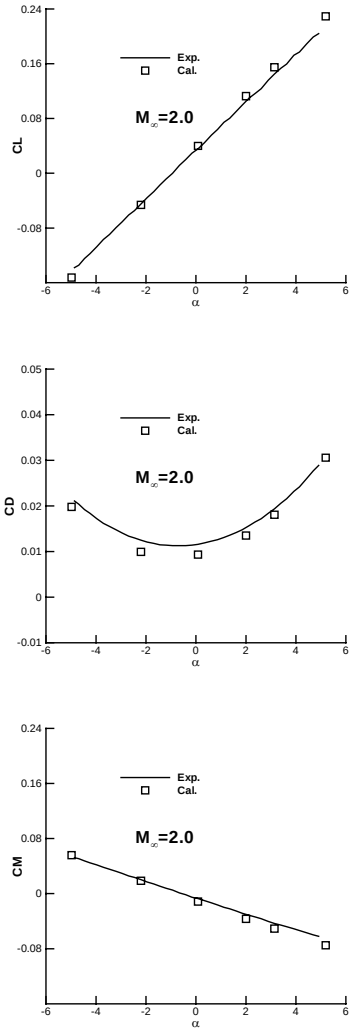


**Fig. 3 The comparison of the predicted lift, drag and pitching moment coefficients with experimental data**

The H-H type multiblock grid with 30 blocks was generated for the SST configuration shown in Fig. 2. The comparison of the predicted coefficients of lift, drag and pitching moment with the experimental data of wind tunnel is depicted in Fig. 3, which agrees each other very well. The cruise lift coefficient at cruise condition of $M_\infty = 2.0$, $\alpha = 2°$ is predicted as $C_{L0} = 0.112$, which is in correspondence with the experimental value of 0.110. For the quasi-steady model equation of motion, the derivative of lift coefficient needs to be known. Based on the lift curve, the derivative can be approximately calculated as $C_{L\alpha} = 2.15$.

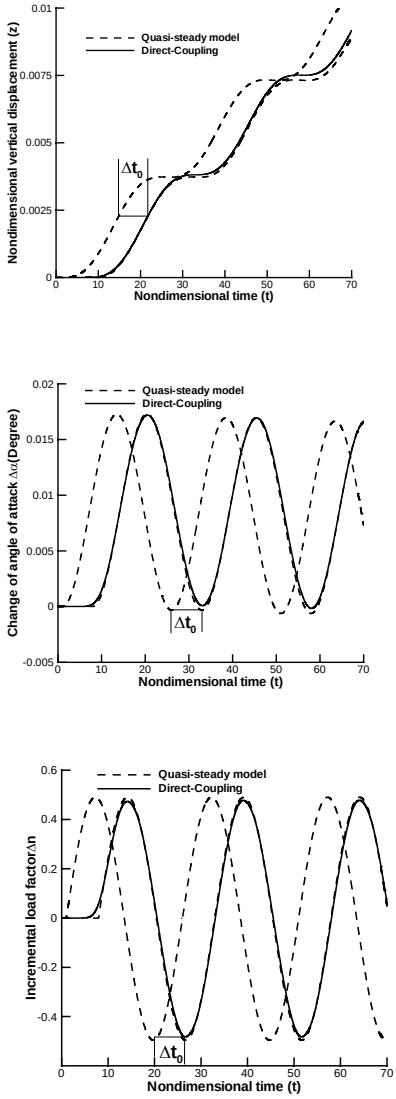


**Fig. 4 Time histories of vertical displacement, change of angle of attack and incremental load factor for SST at** $M_\infty = 2.0$, $\alpha = 2°$

**4.1 Supersonic dynamic response at** $M_\infty = 2.0$

As the aircraft is cruising at $M_\infty = 2.0$, $\alpha = 2°$, a vertical harmonic flow perturbation is added to the aircraft with

$$w(t) = w_0 \sin(\omega t) \qquad (9)$$

The amplitude of the flow perturbation is set to be as $w_0 = 50\,ft/s$ and the reduced frequency $k = \omega c / V_\infty = \pi / 12.5$, which are corresponding to the

design cruise gust speed (the effect of altitude is not considered) and the frequency of one-minus-cosine discrete gust profile [4].

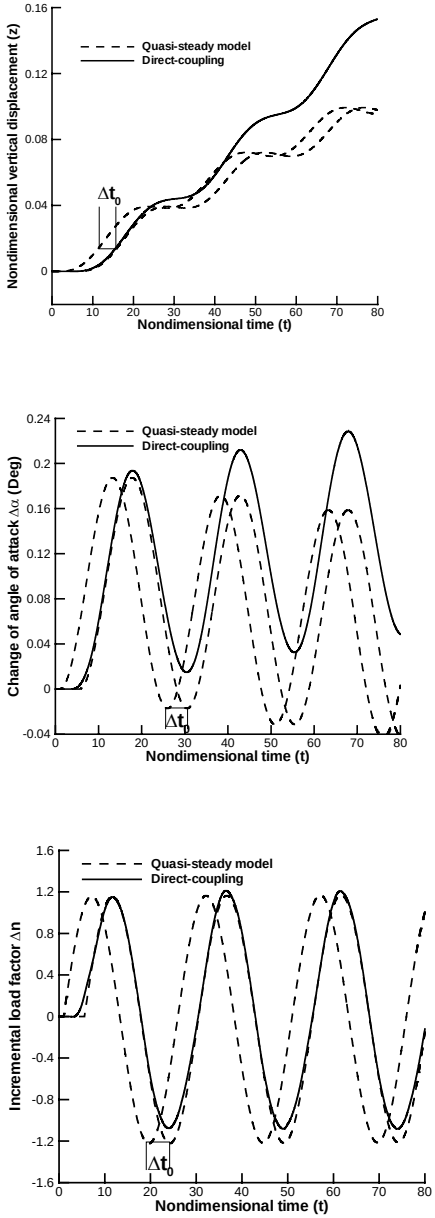


**Fig. 5 Time histories of vertical displacement, angle of attack and incremental load factor for SST at** $M_\infty = 0.9$, $\alpha = 2.14°$

The airplane is assumed as rigid body and only the motion in vertical plunging is considered. Dynamic responses are calculated with the above two methods. For the solution of the equations of motion, the initial conditions are assumed as $z_{t=0} = 0, \dot{z}_{t=0} = 0$ . Fig. 4 shows the time histories of vertical displacement $z(t)$, change of angle of attack due to motion $\Delta\alpha(t) \approx \dot{z}(t)/V_\infty$ and incremental load factor $\Delta n(t) = \ddot{z}(t)/g$ . For the comparison, the dynamic responses of 'quasi-steady model' method after the translation of lag time $t_0 = 6.93$ are also depicted in the figure. If the time lag of the 'quasi-steady model' method can be ignored, the results of the two methods show nearly the same. In fact, the incremental load factor is equivalent to the lift coefficient. It indicates, in this case, the dynamic lift increase due to airplane motion is small and can be neglected.

In the above comparison, although the two methods can be used for dynamic response analyses, the computational expenses are completely different. Comparing the direct-coupling method, the time cost of the quasi-steady method can be ignored, but the method cannot provide any information of flowfield and the corresponding load distribution, and the lag time is unknown before the direct-coupling method is implemented.

### 4.2 Transonic dynamic response at $M_\infty = 0.9$

The SST experimental model is designed for cruise flight at $M_\infty = 2.0$ , $\alpha = 2°$ and the flight altitude of 15,000m. A future SST is expected to cruise at a supersonic speed only over the sea and to cruise at a transonic speed over the land. Due to the strong nonlinearity of transonic flows, the transonic dynamic response may be interested. Therefore, it is assumed that the experimental airplane may cruise at $M_\infty = 0.9$ and the flight altitude of 9,000m. At the cruise flight, due to the equilibrium of various forces and moments, the cruise lift should be equal to the total weight of airplane. From the lift curve at $M_\infty = 0.9$, the cruise angle of attack is estimated as $\alpha = 2.14°$ . The numerical results show the pitching moment about the gravity center of the airplane still exists for this case. In fact, to guarantee the cruise flight of the airplane at transonic Mach number, the high-lift-system and the empennage deflection should be used to keep the equilibrium of forces and moments. In the paper, only the same full aircraft of the above supersonic dynamic analyses is used for the transonic dynamic analyses.

The time histories of dynamic responses are shown in Fig. 5, in which the dynamic responses of the

'quasi-steady model' method after the translation of lag time $t_0 = 4.55$ are also depicted in the figure. Even no consideration of time lag, comparing direct-coupling method, the quasi-steady method predicts the slower growth of displacement with time and the smaller maximum load incremental factor. It indicates the quasi-steady method is unsuitable for the analyses of transonic dynamic responses. In other words, for transonic gust response analyses, the effect of pitching motion should be considered. The direct-coupling method can treat such a problem, while the quasi-steady model method is only suitable for analyses of single freedom motion.

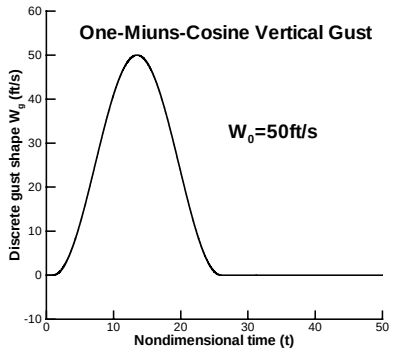


**Fig. 6 One-minus-cosine gust velocity profile**

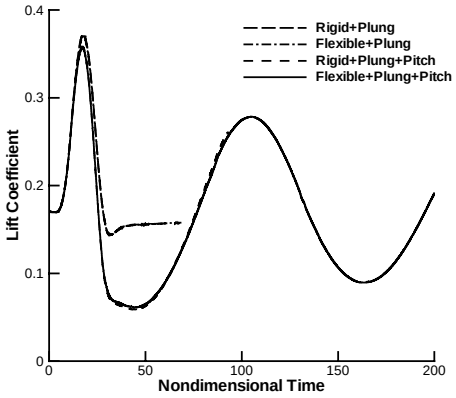


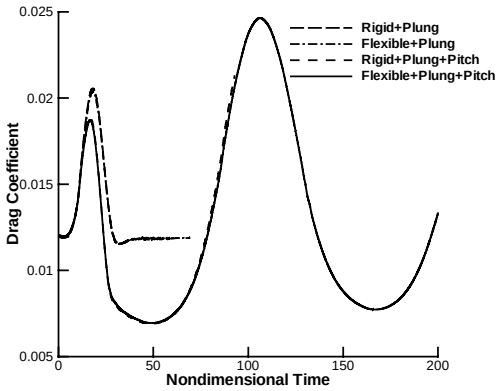


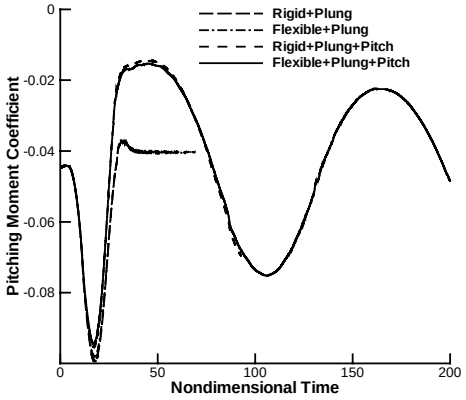


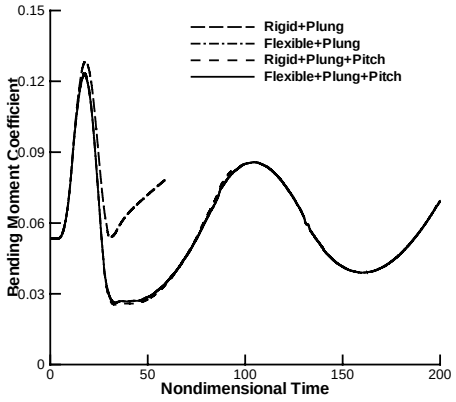


**Fig. 7 Time histories of the coefficients of lift, drag, pitching moment and bending moment for rigid and flexible configurations at** $M_\infty = 0.9$, $\alpha = 2.14°$

### 4.3 Dynamic response for one-minus-cosine gust

The early design methods for gust loads were based on the discrete gust having one-minus-cosine velocity profile, namely,

$$W_g = \frac{1}{2} W_0 \left( 1 - \cos \frac{2\pi x}{2H} \right) \qquad (13)$$

$W_0$ is the design cruise gust velocity, which is specified as 50ft/s at the altitudes from sea level to 20,000ft and then decreases linearly as the functions of altitudes [4]. In the present calculation of cruise altitude of 9,000 m, $W_0$ is assumed as 50ft/s. The gust gradient distance H is taken as the 12.5 times mean geometric chord lengths based on the experimental evidence [4]. Before and after the discrete gust pulse, there is no gust flow perturbation, which velocity profile is shown in Fig. 6. In the following, we need to study how the airplane moves in plunging and pitching, how the loads change and how the structure deforms under the discrete gust profile. For the solution of structural deformation, the data of the structural oscillating natural modes and frequencies based on the wind tunnel model are provided by the NAL. In the paper, total four cases named as 'Rigid+Plung', 'Flexible+Plung' 'Rigid+Plung+Pitch', and 'Flexible+Plung+Pitch' are simulated. The fourth case is the most complicated case, which need to simulate the motion of the aircraft in plunging and pitching with its structural deformation.

The time histories of the load coefficients of lift, drag, pitching moment and bending moment are shown in Fig. 7, which indicates the loads are nearly unchangeable due to the consideration of structural deformation because of the strong structural rigidity of the present SST model airplane. When the airplane flights through the gust pulse, forces and moments also experience a pulse, but a little large maximum load is predicted without the consideration of the motion in pitching. After the pulse response, the loads tend to recover the equilibrium state or emerge to oscillate in decay for the methods with and without the consideration of the motion in pitching.

The displacement in plunging and the angular displacement in pitch are depicted in Fig. 8. Without the consideration of motion in pitching, the displacement in plunging increases very quickly with the time, which is obviously contrary to the fact. So the method neglected pitching motion cannot simulate correctly the response motion of the aircraft. Under the consideration of airplane motion in plunging and pitching, the responses of the airplane appear two freedoms of oscillation. As the airplane plunges up, the airplane pitches down simultaneously, which can be used for the explanation of the change of loads in Fig. 7, namely due to the decrease of angle of attack, the lift, drag and bending moments increase and pitching moment decreases. On the contrary, when the airplane plunges down and pitches up, due to the decrease of angle of attack, the lift, drag and bending moment decrease and the pitching moment increases. The maximum amplitudes of the plunging and pitching oscillation are about 0.1 times mean aerodynamic chord lengths and 1.8 degree, respectively. The numerical results also show that the pitching oscillation decays much faster than that of plunging oscillation.

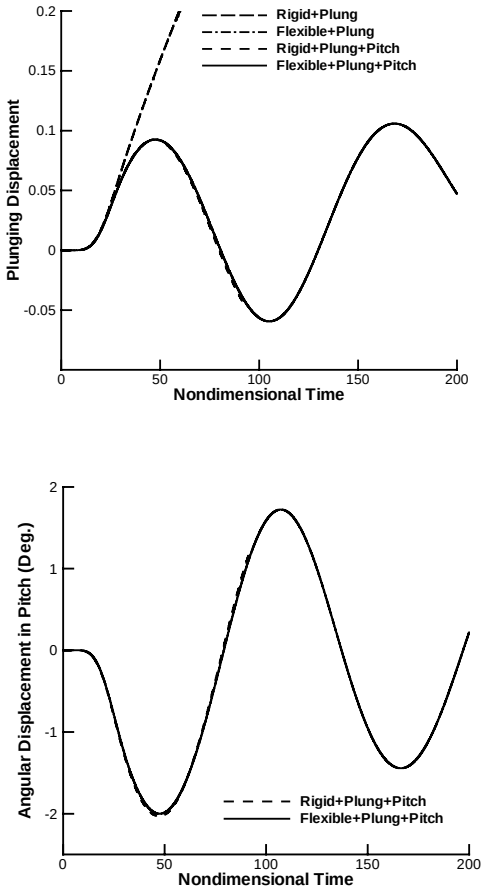


**Fig. 8 Time histories of the vertical plunging displacement and angular displacement in pitch for rigid and flexible configurations at** $M_\infty = 0.9$ , $\alpha = 2.14°$

Due to the structural rigidity of the SST model airplane, the loads and the response motions in plunging and pitching are nearly no differences for rigid and

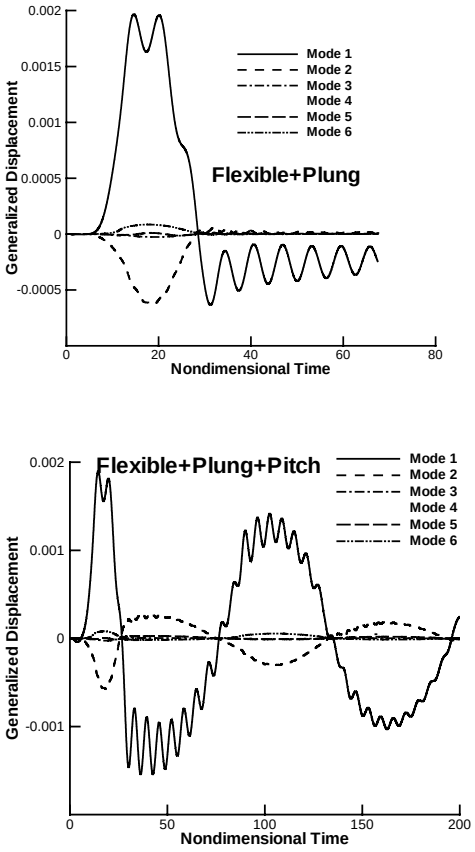


**Fig. 9 Time histories of structural deformation of the first six modes for the flexible configuration with and without the pitching motion at** $M_\infty = 0.9$, $\alpha = 2.14°$

flexible analyses. Fig. 9 gives the time histories of structural deformation of the generalized displacements with and without the consideration of the motion in pitching. For the airplane of rigidity, although the deformation is smaller, the airplane experiences a larger structural deformation in the gust process, which has the same changeable tendency of the loads in Fig. 7. After the pulse response, structural deformation oscillates to revert the original equilibrium state without the consideration of the motion in pitching, and with the consideration of two freedoms of motion, the structural deformation oscillates in much more complicated form, which couples the natural structural oscillation of high frequency and the airplane motion of long period in plunging and pitching. Finally, the dynamic responses of the first two modes with and without the consideration of pitching motion are shown in Fig. 10. Through the comparison, we know both methods can simulate correctly the structural deformation in the process of gust pulse, but complete different process of structural deformation after the gust pulse.

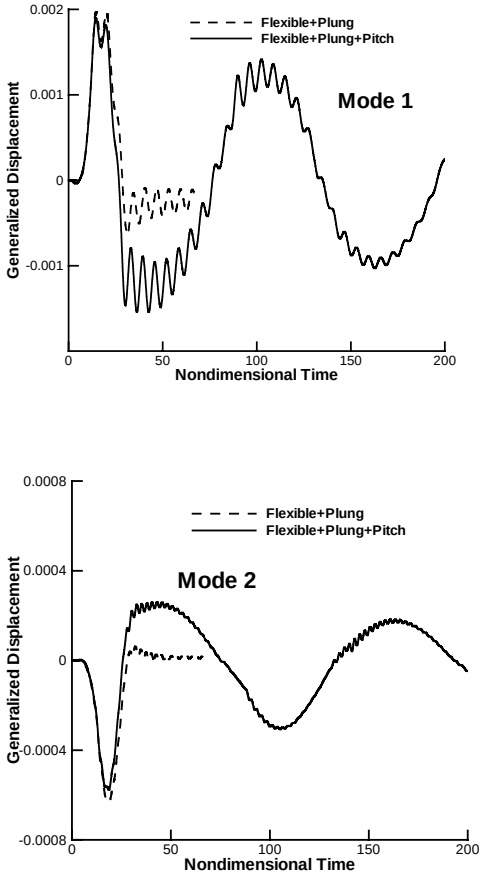


**Fig. 10 The comparison of structural deformation of the first two modes for the flexible configuration with and without the pitching motion at** $M_\infty = 0.9$, $\alpha = 2.14°$

## Conclusion

In the paper, a solver for the analyses of discrete gust response has been developed through the coupling of Navier-Stokes equations and structural and flight dynamic equations of motion. The gust responses for the SST model have been analyzed with the resulting solver. Numerical results indicate the loads and structural deformation experience a larger pulse change in the discrete gust encounter, then the airplane moves in two degrees of freedoms in plunging and pitching oscillations. Without the consideration of the motion in pitching, the time histories of the airplane motion cannot be simulated

correctly. Due to the stronger rigidity for the present SST structural model, there is nearly no any influence for the loads and motions of the aircraft due to the consideration of structural deformation.

**Acknowledgement**

Structural data of SST model were provided by Jiro Nakamichi of National Aerospace Laboratory of Japan.

**References**

[1] B. Perry III, A. S. Pototzky and J. A. Woods: NASA Investigation of a Claimed “Overlap” Between Two Gust Response Analysis Methods, *Journal of Aircraft*, Vol.27, No. 7, 1990, pp.605-611.

[2] R. C. Scott, A. S. Pototzky and B. Perry III: Computation of Maximized Gust Loads for Nonlinear Aircraft Using Matched-Filter-Based Schemes. *Journal of Aircraft*, Vol.30, No. 5, 1993, pp.763-768.

[3] Y. N. Lee and C. E. Lan: Analysis of Random Response with Nonlinear Unsteady Aerodynamics, *Journal of Aircraft*, Vol. 38, 2000, No. 8, pp.1305-1312.

[4] F. M. Hoblit: Gust Loads on Aircraft: Concepts and Application, *AIAA Education Series*, AIAA, Washington, DC, 1988, pp. 29-46.

[5] G. W. Yang, S. Obayashi and J. Nakamichi: Aileron Buzz Simulation Using an Implicit Multiblock Aeroelastic Solver. *Journal of Aircraft*, to appear.

[6] K. Sakata: Supersonic Experimental Airplane Program in NAL and its CFD-Design Research Demand, *2nd SST-CFD-Workshop*, Tokyo, 2000.

[7] P. D. Thomas and C. K. Lombard: Geometric Conservation Law and Its Application to Flow Computations on Moving Grids. *AIAA Journal*, Vol. 17, No. 10, 1979, pp.1030-1037.

[8] B. S. Baldwin and H. Lomax: Thin Layer Approximation and Algebraic Model for Separated Turbulent Flow, *AIAA Paper 78-0257, Jan. 1978*.

[9] S. Yoon and A. Jameson: Lower-Upper Symmetric Gauss Seidel Method for the Euler and Navier-Stokes Equations. *AIAA Journal*, Vol. 26, No. 9, 1988, pp.1025-1026.

[10] S. Obayashi and G. P. Guruswamy: Convergence Acceleration of a Navier-Stokes Solver for Efficient Static Aeroelastic Computations, *AIAA Journal*, Vol.33, No. 6, 1995, pp.1134-1141.

[11] G. W. Yang, M. Kondo and S. Obayashi: Multiblock Navier-Stokes Solver for Wing/Fuselage Transport Aircraft, *JSME International Journal*, Series B, Vol.45, No. 1, 2002, pp.85-90.

[12] R. L. Bisplinghoff, H. Ashley and R. L. Halfman: Aeroelasticity, Addison-Wesley, Reading, Massachusetts, 1955.

[13] G. W. Yang and S. Obayashi: Transonic Aeroelastic Calculation with Full Implicit Subiteration and Deforming Grid Approach, *Aeronautical Numerical Simulation Technology Symposium 2001*, Tokyo, June, 2001.